NeuroImage: Clinical 32 (2021) 102887

Contents lists available at ScienceDirect

NeuroImage: Clinical

journal homepage: www.elsevier.com/locate/ynicl

Examining brain white matter after pediatric mild traumatic brain injury using neurite orientation dispersion and density imaging: An A-CAP study

Ayushi Shukla [a,b,c], Ashley L. Ware [b,c,d], Sunny Guo [d], Bradley Goodyear [c,e,f], Miriam H. Beauchamp [g,h], Roger Zemek [i,j], William Craig [k], Quynh Doan [l], Christian Beaulieu [m], Keith O. Yeates [b,c,d], Catherine Lebel [b,c,n,*], on behalf of the Pediatric Emergency Research Canada A-CAP study team

[a] Cumming School of Medicine, University of Calgary, Canada
[b] Alberta Children's Hospital Research Institute, Canada
[c] Hotchkiss Brain Institute, University of Calgary, Canada
[d] Department of Psychology, University of Calgary, Canada
[e] Seaman Family MR Research Centre, Foothills Medical Centre, Canada
[f] Department of Radiology, University of Calgary, Canada
[g] Department of Psychology, Université de Montreal, Canada
[h] Ste Justine Hospital Research Center, Canada
[i] Department of Pediatrics and Emergency Medicine, University of Ottawa, Canada
[j] Children's Hospital of Eastern Ontario Research Institute, Canada
[k] Department of Pediatrics, University of Alberta and Stollery Children's Hospital, Canada
[l] Department of Pediatrics, University of British Columbia and BC Children's Hospital, Canada
[m] Department of Biomedical Engineering, University of Alberta, Canada
[n] Department of Radiology, University of Calgary, Canada

ARTICLE INFO

Keywords:
Diffusion tensor imaging
Neurite orientation dispersion and density imaging
pediatric mTBI
Mild orthopedic injury

ABSTRACT

Background: Pediatric mild traumatic brain injury (mTBI) affects millions of children annually. Diffusion tensor imaging (DTI) is sensitive to axonal injuries and white matter microstructure and has been used to characterize the brain changes associated with mild traumatic brain injury (mTBI). Neurite orientation dispersion and density imaging (NODDI) is a diffusion model that can provide additional insight beyond traditional DTI metrics, but has not been examined in pediatric mTBI. The goal of this study was to employ DTI and NODDI to gain added insight into white matter alterations in children with mTBI compared to children with mild orthopedic injury (OI).
Methods: Children (mTBI n = 320, OI n = 176) aged 8–16.99 years (12.39 ± 2.32 years) were recruited from emergency departments at five hospitals across Canada and underwent 3 T MRI on average 11 days post-injury. DTI and NODDI metrics were calculated for seven major white matter tracts and compared between groups using univariate analysis of covariance controlling for age, sex, and scanner type. False discovery rate (FDR) was used to correct for multiple comparisons.
Results: Univariate analysis revealed no significant group main effects or interactions in DTI or NODDI metrics. Fractional anisotropy and neurite density index in all tracts exhibited a significant positive association with age and mean diffusivity in all tracts exhibited a significant negative association with age in the whole sample.
Conclusions: Overall, there were no significant differences between mTBI and OI groups in brain white matter microstructure from either DTI or NODDI in the seven tracts. This indicates that mTBI is associated with relatively minor white matter differences, if any, at the post-acute stage. Brain differences may evolve at later stages of injury, so longitudinal studies with long-term follow-up are needed.

* Corresponding author at: Department of Radiology, University of Calgary, 2500 University Drive NW, Calgary, AB T2N 1N4, Canada.
E-mail address: clebel@ucalgary.ca (C. Lebel).

https://doi.org/10.1016/j.nicl.2021.102887
Received 18 August 2021; Received in revised form 26 October 2021; Accepted 16 November 2021
Available online 19 November 2021

Table 1
Demographic data and injury characteristics for sample included in final analysis in the current study.

Variable		mTBI*n* = 319	OI*n* = 176	p test
Age [Mean (SD)]		12.38 (2.42)	12.49 (2.22)	0.619
Full Scale IQ [Mean (SD)]*		105.58 (13.52)	107.66 (13.08)	0.120
PCS				
	Premorbid Somatic	3.05 (4.02)	1.92 (2.79)	0.001
	Premorbid Cognitive	9.43 (7.74)	7.05 (7.03)	0.001
	Post-acute Somatic	6.89 (5.46)	1.38 (2.23)	<0.001
	Post-acute Cognitive	11.64 (0.48)	6.21 (6.85)	<0.001
Site_MRI (%)				0.002
	Calgary-GE	83 (26.0)	37 (21.0)	
	Edmonton-Prisma	81 (25.4)	43 (24.4)	
	Montreal-GE	25 (7.8)	3 (1.7)	
	Montreal-Prisma	14 (4.4)	6 (3.4)	
	Ottawa-Skyra	40 (12.5)	18 (10.2)	
	Vancouver-GE	76 (23.8)	69 (39.2)	
Sex (%)	Male	199 (62.4)	96 (54.5)	0.108
Parental education (%)				0.952
	No certificate, diploma or degree	9 (1.8)	4 (2.3)	
	High school diploma or equivalent	47 (14.7)	22 (12.5)	
	Trades certificate or diploma	33 (10.3)	15 (8.5)	
	2-year college diploma	59 (18.5)	35 (19.8)	
	4-year bachelors degree	101 (31.6)	57 (32.3)	
	Masters degree	33 (10.3)	22 (12.5)	
	Doctoral degree (PhD or similar)	10 (3.1)	4 (2.3)	
	Medical degree	5 (1.5)	4 (2.3)	
	Unknown	22(6.8)	13(7.3)	
Race/Ethnicity (%)				
	White	215 (67.4)	115 (65.3)	
	Asian	27 (8.5)	12 (6.8)	
	Black	13 (4.0)	5 (2.8)	
	Latinx	8 (2.5)	8 (4.5)	
	Indigenous	7 (2.1)	3 (1.7)	
	Other/Mixed	43 (13.5)	29 (16.5)	
	Unknown	6 (1.9)	4 (2.3)	
Mechanism of injury (%)				
	Bicycle related	4 (1.2)	8 (4.5)	
	Fall	114 (35.7)	77 (43.7)	
	Struck object	84 (26.3)	31 (17.6)	
	Struck person	57 (17.8)	19 (10.8)	
	Other	4 (1.2)	11 (6.2)	
	Unknown	56 (17.5)	30 (17.0)	
Sport-related injury	Sports/Recreational Play (%)	230 (84.9)	134 (85.4)	

SD = Standard Deviation; *collected only at 3-month follow-ups (n = 431), measured using two subtests from the Wechsler Abbreviated Scale of Intelligence; PCS = Post concussive symptoms as measured using the Health and Behaviour Inventory (Ayr et al., 2009).

1. Introduction

Traumatic brain injury (TBI) is a global public health concern that affects millions of children annually (Dewan et al., 2018). Seventy-five to ninety percent of all TBIs are mild in severity (Potential Effects, 2019; WHO, 2020). Mild TBI (mTBI) can be associated with ongoing emotional, cognitive, and physical complaints, such as headaches, irritability, and forgetfulness, known as persistent post-concussive symptoms (PPCS) (Arciniegas et al., 2005; Zemek et al., 2016; Ledoux et al.,

Table 2
Table depicting means and standard deviations of DTI (FA, MD) and NODDI (NDI, ODI, FISO) metrics for each tract for both groups (mTBI or OI) examined in this study.

Brain Tract	DTI/NODDI metric	Injury			
		mTBI		OI	
		Mean	Standard deviation	Mean	Standard deviation
AF					
	FA	0.45	0.03	0.45	0.03
	MD ($x10^{-3}$) (mm^2/s)	0.77	0.03	0.08	0.03
	AD ($x10^{-2}$)	0.12	0.02	0.12	0.02
	RD ($x10^{-3}$)	0.57	0.04	0.57	0.04
	NDI	0.56	0.04	0.56	0.04
	ODI	0.27	0.05	0.27	0.03
	FISO	0.07	0.03	0.08	0.03
Cingulum					
	FA	0.44	0.03	0.44	0.03
	MD ($x10^{-3}$) (mm^2/s)	0.80	0.52	0.80	0.03
	AD ($x10^{-2}$)	0.12	0.02	0.12	0.02
	RD ($x10^{-3}$)	0.60	0.04	0.60	0.04
	NDI	0.54	0.05	0.54	0.05
	ODI	0.28	0.03	0.29	0.03
	FISO	0.08	0.04	0.08	0.04
IFOF					
	FA	0.47	0.03	0.47	0.03
	MD ($x10^{-3}$) (mm^2/s)	0.82	0.03	0.82	0.03
	AD ($x10^{-2}$)	0.13	0.02	0.13	0.02
	RD ($x10^{-3}$)	0.59	0.04	0.59	0.04
	NDI	0.53	0.04	0.53	0.04
	ODI	0.24	0.04	0.25	0.03
	FISO	0.08	0.03	0.08	0.03
ILF					
	FA	0.45	0.02	0.46	0.02
	MD ($x10^{-3}$) (mm^2/s)	0.83	0.03	0.83	0.03
	AD ($x10^{-2}$)	0.13	0.02	0.13	0.02
	RD ($x10^{-3}$)	0.60	0.04	0.60	0.04
	NDI	0.52	0.04	0.53	0.04
	ODI	0.25	0.04	0.26	0.03
	FISO	0.09	0.03	0.09	0.03
CST					
	FA	0.51	0.03	0.52	0.03
	MD ($x10^{-3}$) (mm^2/s)	0.78	0.04	0.78	0.04
	AD ($x10^{-2}$)	0.13	0.02	0.13	0.02
	RD ($x10^{-3}$)	0.52	0.06	0.52	0.06
	NDI	0.59	0.03	0.59	0.03
	ODI	0.23	0.06	0.22	0.02
	FISO	0.10	0.04	0.09	0.03
Uncinate					
	FA	0.41	0.03	0.41	0.03
	MD ($x10^{-3}$) (mm^2/s)	0.84	0.02	0.84	0.02
	AD ($x10^{-2}$)	0.12	0.02	0.12	0.02
	RD ($x10^{-3}$)	0.63	0.03	0.63	0.03
	NDI	0.47	0.04	0.47	0.04
	ODI	0.26	0.04	0.27	0.03
	FISO	0.05	0.03	0.06	0.04
CC					
	FA	0.52	0.03	0.53	0.03
	MD ($x10^{-3}$) (mm^2/s)	0.85	0.06	0.85	0.04
	AD ($x10^{-2}$)	0.14	0.02	0.14	0.02
	RD ($x10^{-3}$)	0.56	0.05	0.56	0.05
	NDI	0.55	0.03	0.55	0.04
	ODI	0.22	0.06	0.22	0.02
	FISO	0.12	0.03	0.11	0.03

DTI = Diffusion tensor imaging, NODDI = Neurite orientation dispersion and density index, AF = Arcuate fasciculus, ILF = Inferior longitudinal fasciculus,

IFOF = Inferior fronto-occipital fasciculus, CST = Corticospinal tract, CC = Corpus callosum, FA = Fractional anisotropy, MD = Mean diffusivity, NDI = Neurite density index, ODI = Orientation dispersion index, FISO = Fraction of isotropic water.

2019). In a majority of children with mTBI, symptoms resolve within 4–6 weeks of injury (Torres et al., n.d; Shenton et al., 2012). Yet, up to 30% of injured children continue to experience persistent post concussive symptoms (PPCS) one month or more after injury (Barlow et al., 2015; Taylor et al., 2010).

The rotational and shearing forces from mTBIs can lead to axonal injuries (Büki and Povlishock, 2006; Eierud et al., 2014),which may underlie PPCS and negative outcomes after mTBI (Niogi and Mukherjee, 2010).These injuries are usually not detectible using conventional imaging techniques such as computed tomography (Einarsen et al., 2019); but techniques such as diffusion tensor imaging (DTI) offer promise for greater sensitivity (Eierud et al., 2014). Generally, studies both in the first week and across the first month post-injury (4–20 days post injury) report higher fractional anisotropy (FA) and lower mean diffusivity (MD) in children with mTBI as compared to healthy controls, indicating possible edema (Wilde et al., 2008; Chu et al., 2010; Virji-Babul et al., 2013; Borich et al., 2013; Mayer et al., 2012; Yallampalli et al., 2013; Wu et al., 2010); but findings have been mixed, with some studies finding no changes (Messé et al., 2011) or lower FA (Wu et al., 2018; Yin et al., 2019). Altered FA, globally as well as in specific tracts, at 3–12 months post-injury has been identified in symptomatic children with mTBI, but not asymptomatic children (Mayer et al., 2012; Bartnik-Olson et al., 2014).

Neurite orientation dispersion and density imaging (NODDI) (Zhang et al., 2012) is another diffusion model that provides three metrics with potentially more specificity than traditional DTI: 1) neurite density index (NDI), sensitive to myelin and axonal density (Palacios et al., 2018); 2) orientation dispersion index (ODI), a measure of angular variation or fanning of neurites (Fukutomi et al., 2018); and 3) fraction of the isotropic diffusion compartment (FISO), an estimate of the free water content in the brain that corresponds to the cerebrospinal fluid space (Zhang et al., 2012). No published studies have examined NODDI metrics in pediatric mTBI, but studies in adults have yielded promising results. Adults with mTBI showed lower NDI and higher FISO as compared to those with orthopedic injuries (OIs), predominantly in anterior brain regions, at two weeks post injury, with subsequent decreases in NDI longitudinally (Palacios et al., 2020). In a longitudinal follow-up of concussed college athletes, spatially extensive decreases in NDI and an increase in ODI over time were identified (Churchill et al., 2019). However, pediatric mTBI presents unique physiological characteristics and different recovery mechanisms compared to adults. Children have distinct cerebral metabolisms, different cranial anatomies and biomechanical properties of injury. In addition, neurobehavioral outcomes after mTBI are a confluence of environmental, age, and psychiatric factors (Figaji, 2017; Gioia et al., 2009; Kirkwood et al., 2006; Eme, 2017). These differences highlight the need for neuroimaging studies of mTBI using NODDI specifically in pediatric samples.

The current study sought to investigate white matter alterations following mTBI in children 8–16 years of age at the post-acute stage (2–33 days) of injury using DTI and NODDI as compared to an OI comparison group. We hypothesized that children with mTBI would exhibit higher FA and lower MD in several white matter tracts compared to the OI comparison group. We also expected lower NDI and higher FISO post-injury in the mTBI group as compared to the OI group.

2. Methods

2.1. Study design and procedure

Data were collected as part of Advancing Concussion Assessment in Pediatrics (A-CAP), a larger multi-site longitudinal cohort study of mTBI (Yeates et al., 2017). Children aged 8 to 16.99 years (mean 12.39 ± 2.32) were recruited within 48 h of mTBI or OI in the emergency department (ED) of five hospitals that are members of the Pediatric Emergency Research Canada (PERC) network (Bialy et al., 2018): Alberta Children's Hospital (Calgary), Children's Hospital of Eastern Ontario (Ottawa), Centre Hospitalier Universitaire (CHU) Sainte-Justine (Montreal), Stollery Children's Hospital (Edmonton), and British Columbia Children's Hospital (Vancouver). Children returned for a post-acute assessment that included diffusion MRI around 10 (mean 11.56 ± 5.43) days post-injury. The study was approved by the research ethics board at each site and informed consent/assent was obtained from participants and their parents and guardians. The detailed protocol for the study has been published elsewhere (Yeates et al., 2017).

2.2. Participants

To be eligible for the study, children had to present to the ED within 48 h of injury and at least one parent and the child had to speak and understand English (or French in Montreal and Ottawa). A total of 967 participants were recruited from the ED, 827 returned for the post-acute follow-up, and 628 completed MRI, and scans for 496 children (mTBI n = 320, OI n = 176) passed quality assurance procedures which included examining the MRIs for motion related and other artefacts and were included in the current study. The participants who completed post-acute MRI did not differ in terms of age, sex, or socio-economic status (SES) compared to children who did not return for post-acute follow-up or who returned but did not complete MRI.

2.2.1. Mild TBI

The mTBI group included children who had a blunt head trauma resulting in at least one of the following three criteria, in accordance with the WHO definition of mTBI (Lefevre-Dognin et al., 2021): 1) observed loss of consciousness, 2) a Glasgow coma scale (Teasdale and Jennett, 1974) score of 13 or 14, or 3) one or more acute signs/

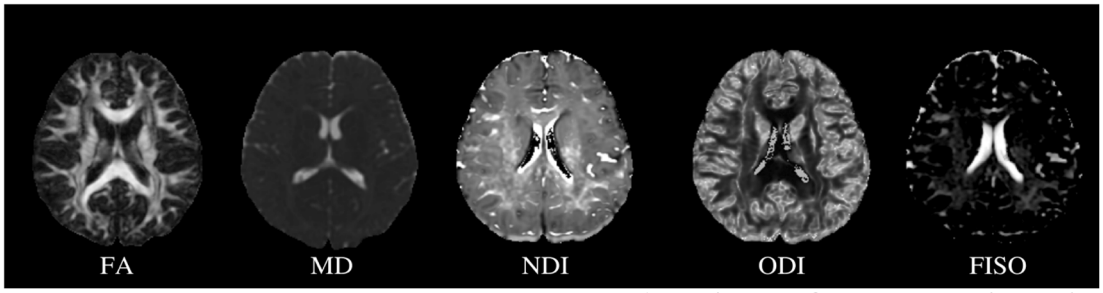

Fig. 1. DTI (FA, MD) and NODDI (NDI, ODI, FISO) metric maps for a representative study participant. DTI = Diffusion tensor imaging, NODDI = Neurite orientation dispersion and density index, FA = Fractional anisotropy, MD = Mean diffusivity, NDI = Neurite density index, ODI = Orientation dispersion index, FISO = Fraction of isotropic water.

Table 3
Fixed-Effects ANOVA results for DTI metrics of 7 tracts (left and right combined). Significant p-values after FDR correction are **bolded**, significant p-values that did not survive FDR correction are *italicized.*

Predictor	F	p-values	q-values	$_{partial}\eta^2$	$_{partial}\eta^2$ 90% CI [LL, UL]
Fractional Anisotropy					
AFmodel: mean_h ~ Injury * dpi_mri * age + sex + Site_MRI					
Injury	0.18	0.673	0.824	0.00	[0.00, 0.01]
dpi_mri	0.00	0.945	0.945	0.00	[0.00, 1.00]
age	**5.46**	**0.020**	**0.023**	**0.00**	**[0.00, 0.03]**
sex	0.07	0.787	0.787	0.00	[0.00, 0.01]
Site_MRI	**106.18**	**<0.001**	**<0.001**	**0.53**	**[0.49, 0.58]**
Injury × dpi_mri	0.26	0.611	0.906	0.00	[0.00, 0.01]
Injury × age	0.09	0.764	1.000	0.00	[0.00, 0.01]
dpi_mri × age	0.03	0.874	1.000	0.00	[0.00, 0.00]
Injury × dpi_mri × age	0.48	0.487	1.000	0.00	[0.00, 0.01]
CCmodel: mean_h ~ Injury * dpi_mri * age + sex + Site_MRI					
Injury	0.41	0.524	0.824	0.00	[0.00, 0.01]
dpi_mri	0.50	0.480	0.840	0.00	[0.00, 0.01]
age	**9.78**	**0.002**	**0.003**	**0.00**	**[0.00, 0.05]**
sex	2.58	0.109	0.254	0.00	[0.00, 0.02]
Site_MRI	**276.19**	**<0.001**	**<0.001**	**0.76**	**[0.72, 0.77]**
Injury × dpi_mri	0.21	0.647	0.906	0.00	[0.00, 0.01]
Injury × age	0.43	0.511	1.000	0.00	[0.00, 0.01]
dpi_mri × age	1.01	0.315	0.635	0.00	[0.00, 0.02]
Injury × dpi_mri × age	0.18	0.669	1.000	0.00	[0.00, 0.01]
Cingulummodel: mean_h ~ Injury * dpi_mri * age + sex + Site_MRI					
Injury	2.21	0.138	0.824	0.00	[0.00, 0.02]
dpi_mri	0.71	0.401	0.840	0.00	[0.00, 0.01]
age	**18.70**	**<0.001**	**<0.001**	**0.06**	**[0.02, 0.07]**
sex	**39.94**	**<0.001**	**<0.001**	**0.06**	**[0.04, 0.12]**
Site_MRI	**121.16**	**<0.001**	**<0.001**	**0.57**	**[0.52, 0.61]**
Injury × dpi_mri	0.76	0.382	0.891	0.00	[0.00, 0.01]
Injury × age	2.33	0.128	0.896	0.00	[0.00, 0.02]
dpi_mri × age	0.83	0.363	0.635	0.00	[0.00, 0.01]
Injury × dpi_mri × age	0.56	0.454	1.000	0.00	[0.00, 0.01]
CSTmodel: mean_h ~ Injury * dpi_mri * sex + age + Site_MRI					
Injury	0.90	0.343	0.824	0.00	[0.00, 0.01]
dpi_mri	0.10	0.756	0.945	0.00	[0.00, 0.01]
sex	0.66	0.418	0.585	0.00	[0.00, 0.01]
age	**68.48**	**<0.001**	**<0.001**	**0.15**	**[0.09, 0.18]**
Site_MRI	**165.52**	**<0.001**	**<0.001**	**0.66**	**[0.60, 0.67]**
Injury × dpi_mri	1.30	0.255	0.891	0.00	[0.00, 0.02]
Injury × sex	0.04	0.843	1.000	0.00	[0.00, 0.01]
dpi_mri × sex	0.23	0.633	1.000	0.00	[0.00, 0.01]
Injury × dpi_mri × sex	0.02	0.899	1.000	0.00	[0.00, 0.00]
IFOFmodel: mean_h ~ Injury * dpi_mri * sex + age + Site_MRI					
Injury	0.68	0.409	0.824	0.00	[0.00, 0.01]
dpi_mri	0.04	0.835	0.945	0.00	[0.00, 0.00]
sex	0.45	0.502	0.586	0.00	[0.00, 0.01]
age	**91.58**	**<0.001**	**<0.001**	**0.14**	**[0.11, 0.21]**
Site_MRI	**173.68**	**<0.001**	**<0.001**	**0.65**	**[0.60, 0.67]**
Injury × dpi_mri	2.39	0.123	0.861	0.00	[0.00, 0.02]
Injury × sex	0.34	0.562	1.000	0.00	[0.00, 0.01]
dpi_mri × sex	1.90	0.169	1.000	0.00	[0.00, 0.02]
Injury × dpi_mri × sex	0.58	0.446	1.000	0.00	[0.00, 0.01]
ILFmodel: mean_h ~ Injury * dpi_mri * age + sex + Site_MRI					
Injury	0.05	0.824	0.824	0.00	[0.00, 0.01]
dpi_mri	0.58	0.448	0.840	0.00	[0.00, 0.01]
age	**13.56**	**<0.001**	**<0.001**	**0.00**	**[0.01, 0.06]**
sex	3.49	0.062	0.217	0.00	[0.00, 0.02]
Site_MRI	**165.60**	**<0.001**	**<0.001**	**0.64**	**[0.59, 0.66]**
Injury × dpi_mri	0.03	0.869	0.992	0.00	[0.00, 0.00]
Injury × age	0.00	0.984	1.000	0.00	[0.00, 1.00]
dpi_mri × age	0.97	0.326	0.635	0.00	[0.00, 0.01]
Injury × dpi_mri × age	0.24	0.623	1.000	0.00	[0.00, 0.01]
UFmodel: mean_h ~ Injury * dpi_mri * age + sex + Site_MRI					
Injury	0.13	0.718	0.824	0.00	[0.00, 0.01]
dpi_mri	0.79	0.375	0.840	0.00	[0.00, 0.01]
age	**5.11**	**0.024**	**0.024**	**0.00**	**[0.00, 0.03]**
sex	1.55	0.214	0.374	0.00	[0.00, 0.02]
Site_MRI	**140.34**	**<0.001**	**<0.001**	**0.59**	**[0.55, 0.63]**
Injury × dpi_mri	0.00	0.992	0.992	0.00	[0.00, 1.00]
Injury × age	0.01	0.903	1.000	0.00	[0.00, 0.00]
dpi_mri × age	1.29	0.257	0.635	0.00	[0.00, 0.02]
Injury × dpi_mri × age	0.06	0.802	1.000	0.00	[0.00, 0.01]
Mean Diffusivity					
AFmodel: mean_h ~ Injury * dpi_mri * age + sex + Site_MRI					
Injury	0.17	0.685	0.749	0.00	[0.00, 0.01]
dpi_mri	1.27	0.261	0.551	0.00	[0.00, 0.02]
age	**35.29**	**<0.001**	**<0.001**	**0.05**	**[0.04, 0.11]**
sex	*5.82*	*0.016*	*0.056*	*0.00*	*[0.00, 0.04]*
Site_MRI	**51.44**	**<0.001**	**<0.001**	**0.38**	**[0.30, 0.41]**
Injury × dpi_mri	0.09	0.770	0.770	0.00	[0.00, 0.01]
Injury × age	0.10	0.755	1.000	0.00	[0.00, 0.01]
dpi_mri × age	1.75	0.186	0.700	0.00	[0.00, 0.02]
Injury × dpi_mri × age	0.11	0.735	1.000	0.00	[0.00, 0.01]
CCmodel: mean_h ~ Injury * dpi_mri * sex + age + Site_MRI					
Injury	0.51	0.477	0.749	0.00	[0.00, 0.01]
dpi_mri	0.52	0.472	0.551	0.00	[0.00, 0.01]
sex	0.17	0.683	0.797	0.00	[0.00, 0.01]
age	**23.03**	**<0.001**	**<0.001**	**0.05**	**[0.02, 0.08]**
Site_MRI	**15.95**	**<0.001**	**<0.001**	**0.15**	**[0.09, 0.19]**
Injury × dpi_mri	0.57	0.452	0.770	0.00	[0.00, 0.01]
Injury × sex	0.34	0.560	1.000	0.00	[0.00, 0.01]
dpi_mri × sex	0.20	0.655	1.000	0.00	[0.00, 0.01]
Injury × dpi_mri × sex	1.46	0.228	1.000	0.00	[0.00, 0.02]
Cingulummodel: mean_h ~ Injury * dpi_mri * sex + age + Site_MRI					
Injury	1.04	0.308	0.749	0.00	[0.00, 0.02]
dpi_mri	0.77	0.380	0.551	0.00	[0.00, 0.01]
sex	0.01	0.941	0.941	0.00	[0.00, 0.00]
age	**19.08**	**<0.001**	**<0.001**	**0.04**	**[0.02, 0.07]**
Site_MRI	**10.73**	**<0.001**	**<0.001**	**0.11**	**[0.06, 0.14]**
Injury × dpi_mri	1.59	0.208	0.770	0.00	[0.00, 0.02]
Injury × sex	0.21	0.649	1.000	0.00	[0.00, 0.01]
dpi_mri × sex	0.25	0.614	1.000	0.00	[0.00, 0.01]
Injury × dpi_mri × sex	0.46	0.497	1.000	0.00	[0.00, 0.01]
CSTmodel: mean_h ~ Injury * dpi_mri * age + sex + Site_MRI					
Injury	0.10	0.749	0.749	0.00	[0.00, 0.01]
dpi_mri	0.69	0.407	0.551	0.00	[0.00, 0.01]
age	**22.60**	**<0.001**	**<0.001**	**0.06**	**[0.02, 0.08]**
sex	1.55	0.213	0.497	0.00	[0.00, 0.02]
Site_MRI	**331.28**	**<0.001**	**<0.001**	**0.78**	**[0.76, 0.80]**
Injury × dpi_mri	0.14	0.708	0.770	0.00	[0.00, 0.01]
Injury × age	0.29	0.592	1.000	0.00	[0.00, 0.01]
dpi_mri × age	1.07	0.300	0.700	0.00	[0.00, 0.02]
Injury × dpi_mri × age	0.45	0.502	1.000	0.00	[0.00, 0.01]
IFOFmodel: mean_h ~ Injury * dpi_mri * sex + age + Site_MRI					
Injury	0.26	0.612	0.749	0.00	[0.00, 0.01]
dpi_mri	1.87	0.173	0.551	0.00	[0.00, 0.02]
sex	0.18	0.675	0.797	0.00	[0.00, 0.01]
age	**112.83**	**<0.001**	**<0.001**	**0.19**	**[0.14, 0.24]**
Site_MRI	**34.97**	**<0.001**	**<0.001**	**0.27**	**[0.21, 0.31]**
Injury × dpi_mri	0.11	0.738	0.770	0.00	[0.00, 0.01]
Injury × sex	0.30	0.583	1.000	0.00	[0.00, 0.01]
dpi_mri × sex	3.63	0.057	0.399	0.00	[0.00, 0.03]
Injury × dpi_mri × sex	0.12	0.731	1.000	0.00	[0.00, 0.01]
ILFmodel: mean_h ~ Injury * dpi_mri * age + sex + Site_MRI					
Injury	0.84	0.359	0.749	0.00	[0.00, 0.01]
dpi_mri	0.64	0.424	0.551	0.00	[0.00, 0.01]
age	**27.72**	**<0.001**	**<0.001**	**0.04**	**[0.03, 0.09]**
sex	**11.00**	**0.001**	**0.007**	**0.00**	**[0.01, 0.05]**

(*continued on next page*)

Table 3 (*continued*)

Predictor	F	p-values	q-values	partial η^2	partial η^2 90% CI [LL, UL]
Site_MRI	**61.19**	**<0.001**	**<0.001**	**0.39**	**[0.33, 0.43]**
Injury × dpi_mri	0.27	0.601	0.770	0.00	[0.00, 0.01]
Injury × age	0.75	0.388	1.000	0.00	[0.00, 0.01]
dpi_mri × age	1.11	0.293	0.700	0.00	[0.00, 0.01]
Injury × dpi_mri × age	0.22	0.641	1.000	0.00	[0.00, 0.01]
UFmodel: mean_h ~ Injury * dpi_mri * age + sex + Site_MRI					
Injury	2.19	0.139	0.749	0.00	[0.00, 0.02]
dpi_mri	0.27	0.607	0.607	0.00	[0.00, 0.01]
age	**11.41**	**0.001**	**0.001**	**0.00**	**[0.01, 0.05]**
sex	0.78	0.379	0.663	0.00	[0.00, 0.01]
Site_MRI	**11.84**	**<0.001**	**<0.001**	**0.10**	**[0.06, 0.15]**
Injury × dpi_mri	1.07	0.302	0.770	0.00	[0.00, 0.01]
Injury × age	1.95	0.164	1.000	0.00	[0.00, 0.02]
dpi_mri × age	0.53	0.469	0.821	0.00	[0.00, 0.01]
Injury × dpi_mri × age	0.86	0.354	1.000	0.00	[0.00, 0.01]

Note. LL and UL represent the lower-limit and upper-limit of the partial η^2 confidence interval, respectively. q-value is the expected proportion of false positives incurred when calling a test significant using FDR correction (Storey and Tibshirani, 2003). DTI = Diffusion tensor imaging, AF = Arcuate fasciculus, ILF = Inferior longitudinal fasciculus, IFOF = Inferior fronto-occipital fasciculus, CST = Corticospinal tract, CC = Corpus callosum, UF = Uncinate fasciculus.

symptoms of concussion (i.e., post-traumatic amnesia, post traumatic seizure, vomiting, headaches, dizziness, changes in mental status) identified in the ED by the medical personnel on a case report form.

2.2.2. Mild OI

The OI group met the following inclusion criteria: 1) fracture, sprain, or strain to the upper or lower extremity from a blunt force trauma, and 2) an Abbreviated Injury Scale (GREENSPAN et al., 1985) (AIS) score of 4 or less. An OI comparison group helps control for premorbid demographic and behavioral risk factors (e.g., attention deficit/hyperactivity disorder (ADHD) and impulsivity are associated with higher risk of injury (Meares et al., 2011; Gerring et al., 1998), as well as for sequelae of injury that are not specific to mild TBI (such as pain, requirement of rest), and thus may better delineate the specific effects of mild TBI on brain white matter structure than a healthy comparison group.

2.2.3. Exclusion criteria

Exclusion criteria for the mTBI group were as follows: 1) delayed neurological deterioration (GCS < 13), 2) need for neurosurgical intervention, or 3) loss of consciousness for more than 30 min or post-traumatic amnesia >24 h. For the mild OI group, exclusion criteria were: 1) Any evidence of head trauma or concussion; 2) injuries requiring surgical intervention or procedural sedation. Both groups had the following exclusion criteria: 1) hypoxia, hypotension, or shock during or following the injury, 2) previous TBI requiring overnight hospital stay, 3) previous concussion within 3 months, 4) pre-existing neurological or neurodevelopmental disorders, 5) hospitalisation for psychiatric deficits within the previous 1 year, 6) sedative medication administered during ED visit, 7) injury accompanied by alcohol and/or drug use, 8) abuse or assault related injuries, 9) absence of legal guardians or child in foster care. Children with contraindications to MRI were included in A-CAP but excluded from the present study because they could not complete MRI.

2.3. Magnetic resonance imaging

Participants completed T1-weighted and diffusion imaging at the post-acute assessment between 2 and 23 days (mean 11.56 ± 5.43) post injury. 75.5% of participants were imaged within 14 days post-injury, with 46% imaged between 7 and 14 days after injury. Images were acquired on a 3 T scanner at each site (General Electric MR750w in Calgary; General Electric MR750 and Siemens Prisma in Montreal, General Electric MR750 in Vancouver; Siemens Prisma in Edmonton; Siemens Skyra in Ottawa).

2.3.1. T1 Acquisition

3D T1-weighted magnetisation prepared rapid acquisition gradient echo (MP RAGE)/ Fast spoiled gradient echo brain volume (FSPGR BRAVO) images with repetition time (TR) = 1880/8.25 ms, echo time (TE) = 2.9/3.16 ms, inversion time (TI) = 948/600 ms, field of view (FOV) = 25.6/24 cm, resolution = 0.8x0.8x0.8 mm isotropic, number of slices = 192, scan time (min:sec) = 4:57/5:28 and a flip angle of 10° were acquired for sites with Siemens/GE scanners respectively.

2.3.2. DTI acquisition

Spin-echo, single-shot echo planar imaging (EPI) was used to acquire DTI images with 5 b = 0 s/mm^2, 30 gradient directions at b = 900 s/mm^2, 30 gradient directions at b = 2000 s/mm^2, FOV = 22/24.2 cm, TR = 6300/12000 ms, TE = 55/98 ms, scan time (min:sec) = 7:08/(7:12x2) and a resolution of 2.2 mm isotropic at sites with Siemens/GE scanners respectively.

2.3.3. Quality control

A detailed explanation of the quality control techniques used in the current study can be found elsewhere (Ware et al., 2021). The T1-weighted image data were manually rated for motion by two trained analysts using a 0–2 ordinal scale with "0" assigned to images with gross artifacts that were considered unusable, a rating of "1" assigned to images with apparent, but minor, artifacts that were acceptable for use, and a "2" assigned to images that were free from visible artifact and were considered to be of excellent quality.

Diffusion images were assessed for motion. Participants whose b = 900 s/mm^2 data had more than 7 (i.e., >25%) volumes rated unusable and/or all b0 images rated unusable were excluded from all analyses. For the remaining participants, volumes with motion were removed before calculation of diffusion parameters, but the participants were still included in analysis.

2.3.4. Image processing

T1- and diffusion-weighted DICOM data were converted into NIfTI format using the dcm2niix tool in MRIcron (publicly available software; https://github.com/rordenlab/dcm2niix), and the bval and bvec files were automatically created from the raw diffusion-weighted DICOM headers. During conversion to NIfTI format, T1-weighted images were automatically reoriented to canonical space.

T1-weighted images were processed on the Advanced Remote Cluster (ARC), a remote Linux computing cluster at the University of Calgary, AB, Canada. Brain extractions of T1-weighted images were obtained using the Advanced Normalization Tools version 3.0.0.0. dev13-ga16cc (compiled January 18, 2019) volume-based cortical thickness estimation pipeline (antsCorticalThickness.sh), with the OASIS pediatric template from the MICCAI 2012 Multi Atlas Challenge (Tustison et al., 2014) used for anatomical reference during skull-stripping.

The diffusion-weighted images (b900 and b2000) were corrected for eddy current distortions, motion artifact, and Gibbs ringing, and were tensor fitted using ExploreDTI v4.8.6 running on MATLAB v8.6.0 R2018a (MathWorks Inc., Natick, MA). Semi-automated deterministic streamline tractography (Reynolds et al., 2019) was performed to delineate fiber tracts from the arcuate fasciculus (AF), cingulum bundle, cortico-spinal tract (CST), corpus callosum (CC), inferior fronto-occipital fasciculus (IFOF), inferior longitudinal fasciculus (ILF), and uncinate fasciculus (UF). DTI and NODDI metrics for each tract were averaged across the left and right hemisphere. The FA map of a representative participant was used to register FA maps of all other participants. All tract regions of interest were drawn on this representative participant and registered to other participants' native space data, and

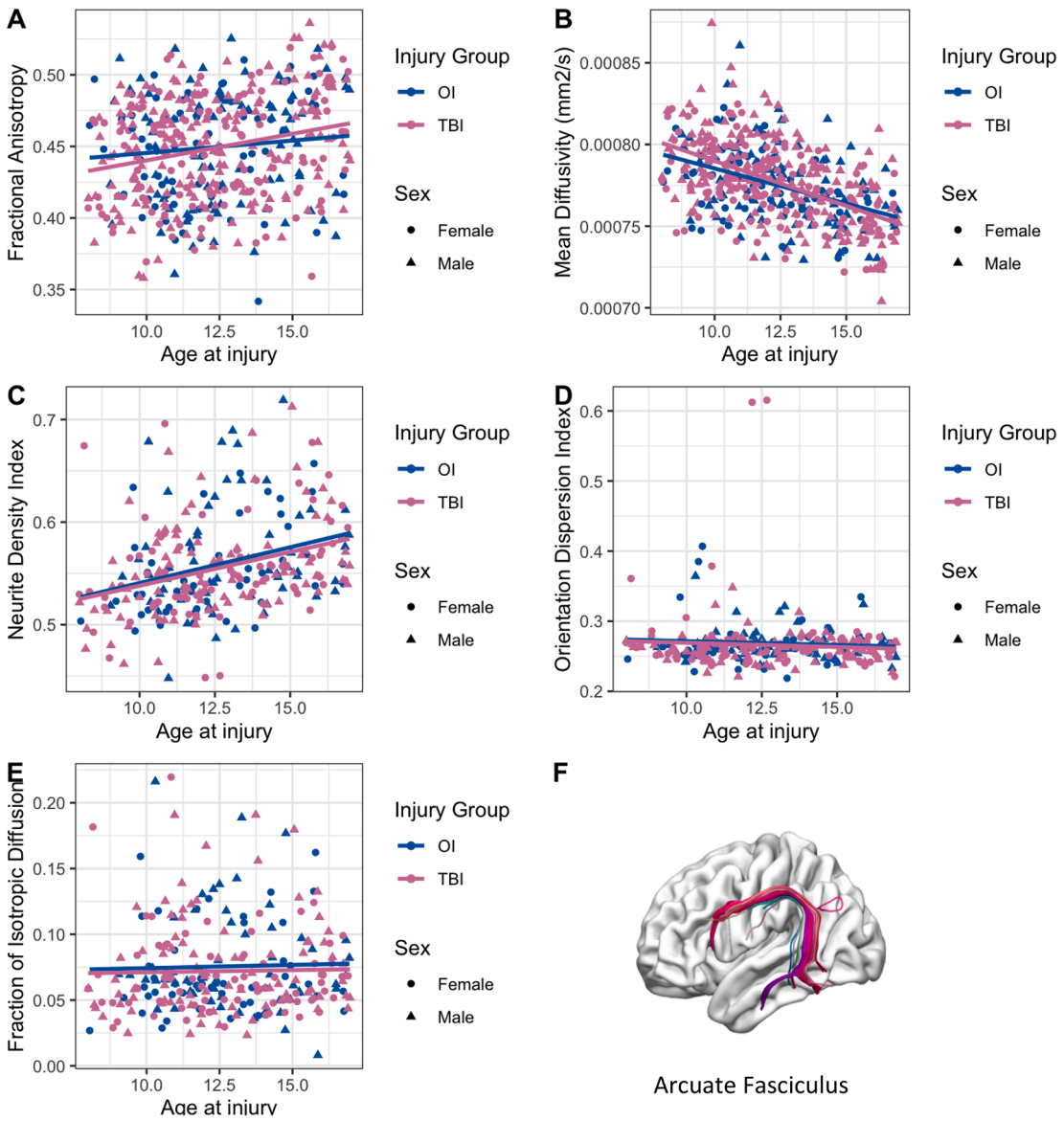

Fig. 2. Scatter plots illustrating relation between age and DTI and NODDI metrics of the left/right combined arcuate fasciculus in children with mTBI and OI. Age-related linear correlations were observed for both groups independently: (A) FA, positive; (B) MD, negative; and (C) NDI, positive. No age-related trends were observed in (D) orientation dispersion index or (E) fraction of isotropic diffusion. (F) is an example of the left arcuate fasciculus tract isolated using semi-automated tractography.

then tractography was performed. Average fractional anisotropy (FA), mean diffusivity (MD), radial diffusivity (RD) and axial diffusivity (AD) values for each tract were calculated for each participant.

Preprocessed data from the ExploreDTI toolbox were exported to the MATLAB NODDI Toolbox (http://www.nitrc.org/projects/noddi_toolbox) and fitted to the NODDI model, obtaining maps of intracellular (f_{icvf} or NDI) and isotropic (FISO) volume fractions and orientation diffusion index (ODI) for each brain tract for which DTI metrics were obtained.

DTI and NODDI metrics were harmonized across scanners using ComBat in R studio; age, injury, and days post-injury were included as covariates during harmonization.

2.3.5. *Statistical analysis*

Demographic data for the sample was examined using analyses of variance (ANOVA) and chi-square tests for continuous and categorical variables, respectively.

As mean DTI and NODDI metric values did not differ between the left and right hemispheres for any tract within each group, metric values were averaged across hemispheres and these averaged values were used in the analysis. Mean metric values for each hemisphere for each metric are noted in Supplementary Table S1.

Univariate analyses of covariance (ANCOVA) were performed to evaluate the relation between white matter metrics (FA, MD, AD, RD, NDI, ODI, FISO) and injury group (mTBI, OI). Because they are known to be associated with DTI and NODDI metrics, and to enable us to investigate their influence on the association between injury group and white matter, age and sex were included in the model as covariates. Days post injury, and scanner type were also included, while controlling for random effect of participant on the analysis. The standard approach for fitting statistical models was followed, with each analysis starting with a full factorial model shown below:

DTI/NODDI metric ~ Group * Days-post injury * Age * Sex + MRI type + (1|Subject)

In cases where the full factorial model did not show best model fit, as determined by significant change in Akaike's Information Criterion and Bayesian Information Criterion (determined using χ^2 comparison tests),

Table 4
Fixed-Effects ANOVA results for NODDI metrics. Significant p-values after FDR correction are **bolded**, significant p-values that did not survive FDR correction are *italicized.*

Predictor	F	p-values	q-values	$_{partial}\eta^2$	$_{partial}\eta^2$90% CI[LL, UL]
Neurite orientation index					
AF					
model: mean_h ~ Injury * dpi * age + sex + Site_MRI					
Injury	2.21	0.138	0.483	0.00	[0.00, 0.04]
days post injury	1.95	0.164	0.287	0.00	[0.00, 0.03]
age	**13.14**	**<0.001**	**<0.001**	**0.06**	**[0.01, 0.10]**
sex	0.01	0.926	0.926	0.00	[0.00, 0.00]
Site_MRI	**27.02**	**<0.000**	**<0.000**	**0.35**	**[0.26, 0.40]**
Injury × days post injury	1.90	0.169	0.394	0.00	[0.00, 0.03]
Injury × age	1.75	0.187	1.000	0.00	[0.00, 0.03]
days post injury × age	2.00	0.159	0.371	0.00	[0.00, 0.03]
Injury × days post injury × age	1.49	0.223	1.000	0.00	[0.00, 0.03]
CC					
model: mean_h ~ Injury * dpi_mri * age + sex + Site_MRI					
Injury	0.49	0.486	0.567	0.00	[0.00, 0.02]
days post injury	2.76	0.098	0.287	0.00	[0.00, 0.04]
age	**11.58**	**0.001**	**0.001**	**0.03**	**[0.01, 0.08]**
sex	1.12	0.290	0.676	0.00	[0.00, 0.03]
Site_MRI	**9.36**	**<0.001**	**<0.001**	**0.14**	**[0.08, 0.20]**
Injury × days post injury	0.58	0.446	0.624	0.00	[0.00, 0.02]
Injury × age	0.26	0.611	1.000	0.00	[0.00, 0.02]
days post injury × age	3.76	0.054	0.189	0.00	[0.00, 0.04]
Injury × days post injury × age	0.27	0.607	1.000	0.00	[0.00, 0.02]
Cingulum					
model: mean_h ~ Injury * dpi_mri * sex + age + Site_MRI					
Injury	1.24	0.266	0.567	0.00	[0.00, 0.03]
days post injury	0.88	0.348	0.406	0.00	[0.00, 0.02]
sex	*6.62*	*0.011*	*0.077*	*0.02*	*[0.00, 0.06]*
age	**5.69**	**0.018**	**0.018**	**0.02**	**[0.00, 0.06]**
Site_MRI	**22.31**	**<0.001**	**<0.001**	**0.29**	**[0.21, 0.35]**
Injury × days post injury	2.12	0.147	0.394	0.00	[0.00, 0.03]
Injury × sex	2.08	0.150	1.000	0.00	[0.00, 0.03]
days post injury × sex	2.25	0.135	0.735	0.00	[0.00, 0.03]
Injury × days post injury × sex	0.66	0.417	1.000	0.00	[0.00, 0.02]
CST					
model: mean_h ~ Injury * dpi_mri * age + sex + Site_MRI					
Injury	0.02	0.881	0.881	0.00	[0.00, 0.01]
days post injury	*5.06*	*0.025*	*0.175*	*0.00*	*[0.00, 0.05]*
age	**23.74**	**<0.001**	**<0.001**	**0.09**	**[0.04, 0.13]**
sex	0.44	0.508	0.889	0.00	[0.00, 0.02]
Site_MRI	**4.34**	**0.001**	**0.001**	**0.09**	**[0.02, 0.11]**
Injury × days post injury	0.04	0.842	0.842	0.00	[0.00, 0.01]
Injury × age	0.07	0.792	1.000	0.00	[0.00, 0.01]
days post injury × age	*5.68*	*0.018*	*0.126*	*0.00*	*[0.00, 0.06]*
Injury × days post injury × age	0.22	0.638	1.000	0.00	[0.00, 0.02]
IFOF					
model: mean_h ~ Injury * dpi_mri * sex + age + Site_MRI					
Injury	0.68	0.411	0.567	0.00	[0.00, 0.02]
days post injury	1.15	0.285	0.399	0.00	[0.00, 0.03]
sex	0.21	0.645	0.903	0.00	[0.00, 0.01]
age	**21.44**	**<0.001**	**<0.001**	**0.06**	**[0.03, 0.12]**
Site_MRI	**16.57**	**<0.001**	**<0.001**	**0.23**	**[0.15, 0.28]**
Injury × days post injury	0.75	0.388	0.624	0.00	[0.00, 0.02]
Injury × sex	0.01	0.934	1.000	0.00	[0.00, 0.00]
days post injury × sex	0.65	0.422	0.868	0.00	[0.00, 0.02]
Injury × days post injury × sex	0.66	0.417	1.000	0.00	[0.00, 0.02]
ILF					
model: mean_h ~ Injury * dpi_mri * sex + age + Site_MRI					
Injury	0.52	0.470	0.567	0.00	[0.00, 0.02]
days post injury	0.18	0.676	0.676	0.00	[0.00, 0.01]
sex	0.01	0.914	0.926	0.00	[0.00, 0.00]
age	**22.11**	**<0.001**	**<0.001**	**0.06**	**[0.03, 0.12]**
Site_MRI	**24.76**	**<0.001**	**<0.001**	**0.31**	**[0.22, 0.36]**
Injury × days post injury	0.37	0.545	0.636	0.00	[0.00, 0.02]
Injury × sex	0.00	0.987	1.000	0.00	[0.00, 1.00]
days post injury × sex	0.46	0.496	0.868	0.00	[0.00, 0.02]
Injury × days post injury × sex	0.47	0.492	1.000	0.00	[0.00, 0.02]
UF					
model: mean_h ~ Injury * dpi_mri * sex + age + Site_MRI					
Injury	2.92	0.088	0.483	0.00	[0.00, 0.04]
days post injury	2.24	0.136	0.287	0.00	[0.00, 0.03]
sex	4.62	0.033	0.115	0.02	[0.00, 0.05]
age	**15.80**	**<0.001**	**<0.001**	**0.05**	**[0.02, 0.10]**
Site_MRI	**12.49**	**<0.001**	**<0.001**	**0.19**	**[0.11, 0.23]**
Injury × days post injury	2.00	0.159	0.394	0.00	[0.00, 0.03]
Injury × sex	0.10	0.747	1.000	0.00	[0.00, 0.01]
days post injury × sex	1.58	0.210	0.735	0.00	[0.00, 0.03]
Injury × days post injury × sex	0.00	0.970	1.000	0.00	[0.00, 1.00]
Orientation dispersion index					
AF					
model: mean_h ~ Injury * dpi_mri * sex + age + Site_MRI					
Injury	0.57	0.453	0.634	0.00	[0.00, 0.02]
days post injury	2.15	0.144	0.336	0.00	[0.00, 0.04]
sex	0.43	0.514	0.68	0.00	[0.00, 0.02]
age	1.30	0.256	0.425	0.00	[0.00, 0.03]
Site_MRI	**18.03**	**<0.001**	**<0.001**	**0.26**	**[0.17, 0.32]**
Injury × days post injury	0.11	0.736	0.883	0.00	[0.00, 0.01]
Injury × sex	0.00	0.955	0.955	0.00	[0.00, 1.00]
days post injury × sex	1.04	0.309	0.541	0.00	[0.00, 0.03]
Injury × days post injury × sex	0.10	0.757	0.968	0.00	[0.00, 0.01]
CC					
model: mean_h ~ Injury * dpi_mri * age * sex + Site_MRI					
Injury	1.58	0.211	0.369	0.00	[0.00, 0.03]
days post injury	2.43	0.120	0.336	0.02	[0.00, 0.04]
age	3.17	0.076	0.266	0.02	[0.00, 0.04]
sex	*5.97*	*0.015*	*0.084*	*0.02*	*[0.00, 0.06]*
Site_MRI	1.33	0.253	0.253	0.02	[0.00, 0.04]
Injury × days post injury	1.23	0.268	0.822	0.00	[0.00, 0.03]
Injury × age	1.56	0.213	0.745	0.00	[0.00, 0.03]
days post injury × age	2.28	0.132	0.462	0.02	[0.00, 0.04]
Injury × sex	*5.52*	*0.019*	*0.066*	*0.02*	*[0.00, 0.06]*
days post injury × sex	*4.58*	*0.033*	*0.136*	*0.02*	*[0.00, 0.05]*
age × sex	*5.07*	*0.025*	*0.122*	*0.02*	*[0.00, 0.05]*
Injury × days post injury × age	1.11	0.293	1.000	0.00	[0.00, 0.03]
Injury × days post injury × sex	*5.41*	*0.021*	*0.073*	*0.02*	*[0.00, 0.06]*
Injury × age × sex	*5.00*	*0.026*	*0.091*	*0.02*	*[0.00, 0.05]*
days post injury × age × sex	3.79	0.053	0.203	0.02	[0.00, 0.05]
Injury × days post injury × age × sex	4.61	0.033	0.115	0.02	[0.00, 0.05]
Cingulum					
model: mean_h ~ Injury * dpi_mri * sex + age + Site_MRI					
Injury	1.63	0.203	0.369	0.00	[0.00, 0.03]

(*continued on next page*)

Table 4 (*continued*)

Predictor	F	p-values	q-values	partial η^2	partial η^2 90% CI[LL, UL]
days post injury	0.20	0.654	0.654	0.00	[0.00, 0.01]
sex	*4.14*	*0.043*	*0.100*	*0.00*	*[0.00, 0.05]*
age	1.68	0.197	0.425	0.00	[0.00, 0.03]
Site_MRI	**11.04**	**<0.001**	**<0.001**	**0.15**	**[0.09, 0.22]**
Injury × days post injury	0.52	0.470	0.822	0.00	[0.00, 0.02]
Injury × sex	0.01	0.916	0.955	0.00	[0.00, 0.00]
days post injury × sex	1.76	0.186	0.434	0.00	[0.00, 0.03]
Injury × days post injury × sex	0.29	0.588	0.968	0.00	[0.00, 0.02]
CST					
model: mean_h ~ Injury * dpi_mri * age * sex + Site_MRI					
Injury	1.67	0.198	0.369	0.00	[0.00, 0.03]
days post injury	*4.36*	*0.038*	*0.266*	*0.02*	*[0.00, 0.05]*
age	*5.56*	*0.019*	*0.133*	*0.02*	*[0.00, 0.06]*
sex	*5.14*	*0.024*	*0.084*	*0.02*	*[0.00, 0.05]*
Site_MRI	**2.58**	**0.027**	**0.031**	**0.04**	**[0.00, 0.08]**
Injury × days post injury	1.18	0.278	0.822	0.00	[0.00, 0.03]
Injury × age	1.59	0.209	0.745	0.00	[0.00, 0.03]
days post injury × age	*3.92*	*0.049*	*0.343*	*0.02*	*[0.00, 0.05]*
Injury × sex	*6.07*	*0.014*	*0.066*	*0.02*	*[0.00, 0.06]*
days post injury × sex	*4.30*	*0.039*	*0.136*	*0.02*	*[0.00, 0.05]*
age × sex	*4.48*	*0.035*	*0.122*	*0.02*	*[0.00, 0.05]*
Injury × days post injury × age	1.04	0.308	1.000	0.00	[0.00, 0.03]
Injury × days post injury × sex	*5.66*	*0.018*	*0.073*	*0.02*	*[0.00, 0.06]*
Injury × age × sex	*5.55*	*0.019*	*0.091*	*0.02*	*[0.00, 0.06]*
days post injury × age × sex	3.63	0.058	0.203	0.02	[0.00, 0.04]
Injury × days post injury × age × sex	*4.90*	*0.028*	*0.115*	*0.02*	*[0.00, 0.05]*
IFOF					
model: mean_h ~ Injury * dpi_mri * sex + age + Site_MRI					
Injury	0.01	0.915	0.939	0.00	[0.00, 0.00]
days post injury	1.08	0.300	0.420	0.00	[0.00, 0.02]
sex	0.30	0.583	0.680	0.00	[0.00, 0.02]
age	0.91	0.342	0.425	0.00	[0.00, 0.02]
Site_MRI	**20.09**	**<0.001**	**<0.001**	**0.27**	**[0.18, 0.32]**
Injury × days post injury	0.02	0.883	0.883	0.00	[0.00, 0.01]
Injury × sex	0.02	0.888	0.955	0.00	[0.00, 0.01]
days post injury × sex	0.65	0.422	0.552	0.00	[0.00, 0.02]
Injury × days post injury × sex	0.10	0.749	0.968	0.00	[0.00, 0.01]
ILF					
model: mean_h ~ Injury * dpi_mri * sex + age + Site_MRI					
Injury	0.01	0.939	0.939	0.00	[0.00, 0.00]
days post injury	0.48	0.490	0.572	0.00	[0.00, 0.02]
sex	0.10	0.752	0.752	0.00	[0.00, 0.01]
age	0.38	0.540	0.540	0.00	[0.00, 0.02]
Site_MRI	**17.82**	**<0.001**	**<0.001**	**0.24**	**[0.16, 0.30]**
Injury × days post injury	0.03	0.854	0.883	0.00	[0.00, 0.01]
Injury × sex	0.10	0.758	0.955	0.00	[0.00, 0.01]
days post injury × sex	0.52	0.473	0.552	0.00	[0.00, 0.02]
Injury × days post injury × sex	0.00	0.968	0.968	0.00	[0.00, 1.00]
UF					
model: mean_h ~ Injury * dpi_mri * sex + age + Site_MRI					
Injury	2.02	0.156	0.369	0.00	[0.00, 0.03]
days post injury	1.48	0.224	0.392	0.00	[0.00, 0.03]
sex	0.96	0.327	0.572	0.00	[0.00, 0.02]
age	0.83	0.364	0.425	0.00	[0.00, 0.02]
Site_MRI	**14.01**	**<0.001**	**<0.001**	**0.21**	**[0.12, 0.25]**
Injury × days post injury	0.68	0.411	0.822	0.00	[0.00, 0.02]
Injury × sex	0.24	0.625	0.955	0.00	[0.00, 0.02]

Table 4 (*continued*)

Predictor	F	p-values	q-values	partial η^2	partial η^2 90% CI[LL, UL]
days post injury × sex	0.19	0.662	0.662	0.00	[0.00, 0.01]
Injury × days post injury × sex	0.00	0.946	0.968	0.00	[0.00, 1.00]
Fraction of isotropic diffusion					
AF					
model: mean_h ~ Injury * dpi_mri * age + sex + Site_MRI					
Injury	3.81	0.052	0.240	0.00	[0.00, 0.05]
days post injury	0.09	0.759	0.759	0.00	[0.00, 0.01]
age	0.08	0.775	0.904	0.00	[0.00, 0.01]
sex	0.80	0.371	0.649	0.00	[0.00, 0.02]
Site_MRI	**2.49**	**0.032**	**0.045**	**0.05**	**[0.00, 0.08]**
Injury × days post injury	*4.30*	*0.039*	*0.247*	*0.00*	*[0.00, 0.05]*
Injury × age	3.34	0.069	0.483	0.00	[0.00, 0.04]
days post injury × age	0.04	0.847	1.000	0.00	[0.00, 0.01]
Injury × days post injury × age	3.82	0.052	0.322	0.00	[0.00, 0.05]
CC					
model: mean_h ~ Injury * dpi_mri * age + sex + Site_MRI					
Injury	2.68	0.103	0.240	0.00	[0.00, 0.04]
days post injury	0.49	0.484	0.759	0.00	[0.00, 0.02]
age	0.00	0.958	0.958	0.00	[0.00, 1.00]
sex	2.89	0.090	0.210	0.00	[0.00, 0.04]
Site_MRI	**11.21**	**<0.001**	**<0.001**	**0.18**	**[0.10, 0.22]**
Injury × days post injury	3.11	0.079	0.247	0.00	[0.00, 0.04]
Injury × age	2.00	0.159	0.556	0.00	[0.00, 0.03]
days post injury × age	0.45	0.502	1.000	0.00	[0.00, 0.02]
Injury × days post injury × age	2.21	0.138	0.322	0.00	[0.00, 0.03]
Cingulum					
model: mean_h ~ Injury * dpi_mri * sex + age + Site_MRI					
Injury	0.91	0.340	0.389	0.00	[0.00, 0.02]
days post injury	0.13	0.715	0.759	0.00	[0.00, 0.01]
sex	3.84	0.051	0.170	0.03	[0.00, 0.05]
age	3.82	0.052	0.353	0.03	[0.00, 0.05]
Site_MRI	**8.65**	**<0.001**	**<0.001**	**0.14**	**[0.07, 0.19]**
Injury × days post injury	1.36	0.244	0.342	0.00	[0.00, 0.03]
Injury × sex	0.57	0.453	1.000	0.00	[0.00, 0.02]
days post injury × sex	1.04	0.310	1.000	0.00	[0.00, 0.03]
Injury × days post injury × sex	0.30	0.585	1.000	0.00	[0.00, 0.02]
CST					
model: mean_h ~ Injury * dpi_mri * age + sex + Site_MRI					
Injury	0.74	0.389	0.389	0.00	[0.00, 0.02]
days post injury	1.07	0.301	0.759	0.00	[0.00, 0.03]
age	0.60	0.441	0.617	0.00	[0.00, 0.02]
sex	0.07	0.792	0.792	0.00	[0.00, 0.01]
Site_MRI	**134.41**	**<0.001**	**<0.001**	**0.71**	**[0.66, 0.74]**
Injury × days post injury	0.52	0.472	0.472	0.00	[0.00, 0.02]
Injury × age	0.53	0.468	0.819	0.00	[0.00, 0.02]
days post injury × age	0.78	0.377	1.000	0.00	[0.00, 0.02]
Injury × days post injury × age	0.26	0.611	1.000	0.00	[0.00, 0.02]
IFOF					
model: mean_h ~ Injury * dpi_mri * sex + age + Site_MRI					
Injury	1.13	0.290	0.389	0.00	[0.00, 0.03]
days post injury	0.34	0.558	0.759	0.00	[0.00, 0.02]
sex	0.08	0.774	0.792	0.00	[0.00, 0.01]
age	2.71	0.101	0.353	0.00	[0.00, 0.04]
Site_MRI	1.58	0.166	0.166	0.05	[0.00, 0.05]
Injury × days post injury	0.89	0.346	0.404	0.00	[0.00, 0.02]
Injury × sex	0.27	0.601	1.000	0.00	[0.00, 0.02]
	0.00	0.996	1.000	0.00	[0.00, 1.00]

(*continued on next page*)

Table 4 (*continued*)

Predictor	F	p-values	q-values	partial η^2	partial $\eta^2$90% CI[LL, UL]
days post injury × sex					
Injury × days post injury × sex	1.12	0.291	1.000	0.00	[0.00, 0.03]
ILF					
model: mean_h ~ Injury * dpi_mri * sex + age + Site_MRI					
Injury	1.45	0.229	0.389	0.00	[0.00, 0.03]
days post injury	0.92	0.338	0.759	0.00	[0.00, 0.02]
age	1.79	0.182	0.425	0.00	[0.00, 0.03]
sex	0.40	0.529	0.741	0.00	[0.00, 0.02]
Site_MRI	1.72	0.130	0.151	0.04	[0.00, 0.05]
Injury × days post injury	2.63	0.106	0.247	0.00	[0.00, 0.04]
Injury × age	1.29	0.257	0.599	0.00	[0.00, 0.03]
days post injury × age	1.26	0.262	1.000	0.00	[0.00, 0.03]
Injury × days post injury × age	2.50	0.115	0.322	0.00	[0.00, 0.04]
UF					
model: mean_h ~ Injury * dpi_mri * sex + age + Site_MRI					
Injury	3.03	0.083	0.240	0.00	[0.00, 0.04]
days post injury	1.41	0.236	0.759	0.00	[0.00, 0.03]
sex	*4.45*	*0.036*	*0.178*	*0.03*	*[0.00, 0.05]*
age	0.83	0.364	0.617	0.00	[0.00, 0.02]
Site_MRI	**6.76**	**<0.001**	**<0.001**	**0.11**	**[0.04, 0.15]**
Injury × days post injury	1.77	0.184	0.322	0.00	[0.00, 0.03]
Injury × sex	0.11	0.739	1.000	0.00	[0.00, 0.01]
days post injury × sex	0.63	0.429	1.000	0.00	[0.00, 0.02]
Injury × days post injury × sex	0.00	0.984	1. 000	0.00	[0.00, 1.00]

Note. LL and UL represent the lower-limit and upper-limit of the partial η^2 confidence interval, respectively. q-value is the expected proportion of false positives incurred when calling a test significant using FDR correction (Storey and Tibshirani, 2003). NODDI = Neurite Orientation Dispersion and Density imaging, AF = Arcuate fasciculus, ILF = Inferior longitudinal fasciculus, IFOF = Inferior fronto-occipital fasciculus, CST = Corticospinal tract, CC = Corpus callosum, UF = Uncinate fasciculus.

the best fitting model was used for data analysis. To correct for 7 comparisons (7 tracts) for each metric, a false discovery rate (FDR) (Benjamini, 1995) correction with a threshold of $q < 0.05$ was used.

Power analysis using G*power 3.1 (Faul et al., 2009) revealed that at a small ($f = 0.10$), medium ($f = 0.25$), and large ($f = 0.40$) effect size f our study has a power of 0.66, 0.99, 1.00 respectively at critical $F = 3.85$ with $\alpha = 0{\cdot}05$ with our sample size $n = 560$.

3. Results

Sample demographics are presented in Table 1. The groups did not differ in age, sex, or Full-Scale IQ. Mean and standard deviations of DTI (FA, MD) and NODDI (NDI, ODI, FISO) metrics for each group (mTBI and OI) are listed in Table 2. Metric maps for each metric for a representative study participant are depicted in Fig. 1.

3.1. DTI

Univariate ANCOVA results examining group differences in DTI metrics are presented in Table 3 (FA, MD) and Supplementary Table S2 (AD, RD). Children with mTBI or OI did not significantly differ on any DTI metric for any of the tracts examined in the current study after FDR correction.

In line with previous research (Reynolds et al., 2019; Deoni et al., 2016); FA in all tracts exhibited a significant positive association with age while MD in all tracts had a significant negative association with age for both injury groups (Table 3, Fig. 2*a, b)*. FA in the cingulum ($p < .001$) and MD in the ILF ($p = .001$) was significantly associated with sex after FDR correction. (Table 3*)*. Post-hoc analysis revealed higher FA in the cingulum and higher MD in the ILF in males as compared to females for both injury groups.

3.2. NODDI

Results from the univariate ANOVA examining group differences on NODDI metrics (NDI, ODI, FISO) are presented in Table 4. No significant differences between children with mTBI and OI were identified on any NODDI metric, before or after FDR correction.

In line with previous research (Geeraert et al., 2019; Mah et al., 2017; Zhao et al., 2021); NDI was significantly positively associated with age in all tracts examined, whereas no significant associations were identified between ODI or FISO and age (Table 4, Fig. 2c, d, e).

4. Discussion

In this large prospective study of children with mTBI, we found no significant differences in diffusion parameters within white matter tracts at the post-acute stage of injury compared to children with orthopedic injuries. This suggests that changes to brain microstructure may not be apparent in the first few weeks following mTBI.

Some previous studies of pediatric mTBI have identified widespread white matter alterations at the post-acute period of injury (Mayer et al., 2012; Babcock et al., 2015; Wilde et al., 2008), whereas others have reported no significant differences in DTI metrics between children with mTBI and controls (Goodrich-Hunsaker et al., 2018; Wilde et al., 2018). This heterogeneity in findings can likely be attributed to small sample sizes (n = 6–83), (Virji-Babul et al., 2013; Churchill et al., 2019; Wilde et al., 2008)narrow (14–17 years) (Yallampalli et al., 2013) or very wide (10–38 years) age ranges (Babcock et al., 2015; Wilde et al., 2018), different comparison groups between studies (OI versus uninjured controls) (Mayer et al., 2012; Palacios et al., 2020; Churchill et al., 2019; Babcock et al., 2015), and differing image analysis techniques (e.g., voxel-wise (Chu et al., 2010; Lancaster et al., 2016), tract based special statistics (Fakhran et al., 2014); whole brain histogram analysis (Delic et al., 2016); deterministic tractography (King et al., 2019; Mac Donald et al., 2018); probabilistic tractography (Manning, 2017). To address the above-mentioned factors that lead to heterogeneity in studies of pediatric mTBI, the current study included a sample size large enough to provide sufficient power to detect small effects ($f = 0.10$), an age range (8–16.99 years) suitable for successful completion of MRI scans while limiting developmental heterogeneity, and an OI comparison group to control for premorbid behavioral differences between children with mTBI and uninjured controls as well as post-injury factors such as stress, pain, and medication effects (Wilde et al., 2018). Therefore, our lack of findings here in multiple brain areas may represent a true lack of measurable changes in white matter structure in children with mTBI at the post-acute injury stage.

We identified a positive association of NDI with age in all tracts examined here, in line with prior work showing that NODDI metrics are more strongly associated with age compared to the DTI metrics of FA, MD, AD and RD (Mah et al., 2017; Genc et al., 2017). However, no differences in NODDI metrics were identified between children with mTBI versus OI in any of the tracts examined. Previous NODDI studies of mTBI in adults have reported lower NDI and higher FISO after mTBI as compared to OI 2-weeks post injury, with decreases in NDI longitudinally (Palacios et al., 2020; Churchill et al., 2019; Churchill et al., 2017). MTBI leads to a neurometabolic cascade beginning with ionic flux and glutamate release at early stages of injury, followed by cytoskeletal damage, axonal dysfunction, and altered neurotransmission, which may lead to inflammation and possible cell death (Giza and Hovda, 2014). The trajectory of these metabolic changes in children differs from that in adults due to higher vulnerability of the younger brain to biomechanical effects after concussion (Post et al., 2017), making the trajectory of white matter changes post-injury different between the pediatric and

adult population, which may explain the lack of differences between the two groups here. Alternatively, in children, white matter alterations after mTBI may not be evident post-acutely and rather may evolve over the course of injury and be observed at a later stage in injury, indicating a need for longitudinal follow-up studies.

An important consideration while interpreting the lack of differences in white matter microstructure between injury groups in this study is the severity or presence of PCS within in the mTBI group. There may be a subgroup within the mTBI group with more severe PCS as compared to the rest of the mTBI group, which may exhibit altered white matter microstructure at the post-acute stage of injury, but these differences may be lost due to the inclusion of the whole mTBI sample, instead of a subset of children. Therefore, examining PCS and their association with white matter microstructure is an important future direction.

Pediatric mTBIs have multiple mechanisms of injury (Haarbauer-Krupa et al., 2018) and lead to diffuse axonal injuries, causing widespread disruptions in brain white matter connectivity (Raizman et al., 2020; Iraji et al., 2016). A graph theory or connectome-based approach to map white matter networks after injury is well suited to characterize these disruptions. Therefore, future studies employing network-based approaches in addition to the currently used structural metrics may yield further insight into pediatric mTBI.

4.1. Limitations

The results from this study should be viewed in light of some limitations. The data were collected at multiple sites across Canada to enable the recruitment of a large study sample. Protocols were standardized, but differences in scan parameters, scanner manufacturers, and sites may introduce confounding factors to images (Palacios et al., 2017). To account for this, we harmonized data using ComBat. We did not obtain pre-injury baseline scans due to methodological limitations; therefore, it cannot be concluded whether the DTI and NODDI metrics observed in this study were a result of injury or are related to pre-injury factors. However, using children with mild OI as the comparison group enabled us to to control for factors that predispose children to injuries, as well as biological and behavioral characteristics (brain changes, pain, etc.) that are caused by injuries in general.

4.2. Conclusions

The current study extends our understanding of white matter microstructure at the post-acute stage of pediatric mild TBI. White matter characteristics post-acutely after injury were similar between children with mTBI and OI, suggesting that differences in the biophysical properties of white matter tracts are not apparent at the post-acute stage of mTBI. Using an OI comparison group in the current study enabled us to control for some common confounding factors that blur comparisons of mTBI to healthy children. White matter differences following mTBI in children may emerge over time, so longitudinal studies are needed, as are analyses of the association between neuroimaging data and PCS.

CRediT authorship contribution statement

Ayushi Shukla: Conceptualization, Data curation, Formal analysis, Methodology, Visualization, Writing – original draft. **Ashley L. Ware:** Data curation, Formal analysis, Writing – review & editing. **Sunny Guo:** Visualization, Writing – review & editing. **Bradley Goodyear:** Conceptualization, Writing – review & editing. **Miriam H. Beauchamp:** Conceptualization, Writing – review & editing. **Roger Zemek:** Conceptualization, Writing – review & editing. **William Craig:** Conceptualization, Writing – review & editing. **Quynh Doan:** Conceptualization, Writing – review & editing. **Christian Beaulieu:** Conceptualization, Writing – review & editing. **Keith O. Yeates:** Conceptualization, Methodology, Funding acquisition, Resources, Supervision, Writing – review & editing. **Catherine Lebel:** Conceptualization, Methodology, Project administration, Resources, Supervision, Writing – review & editing.

Declaration of Competing Interest

The authors declare that they have no known competing financial interests or personal relationships that could have appeared to influence the work reported in this paper.

Appendix A. Supplementary data

Supplementary data to this article can be found online at https://doi.org/10.1016/j.nicl.2021.102887.

References

Dewan, M.C., Rattani, A., Gupta, S., Baticulon, R.E., Hung, Y.-C., Punchak, M., Agrawal, A., Adeleye, A.O., Shrime, M.G., Rubiano, A.M., Rosenfeld, J.V., Park, K.B., 2018. Estimating the global incidence of traumatic brain injury. J. Neurosurg. 130 (4), 1080–1097. https://doi.org/10.3171/2017.10.JNS17352.

Potential Effects | Concussion | Traumatic Brain Injury | CDC Injury Center. (2019, February 25). https://www.cdc.gov/traumaticbraininjury/outcomes.html.

WHO | Neurological Disorders: Public Health Challenges (n.d.). Retrieved July 27 2020 https://www.who.int/mental_health/publications/neurological_disorders_ph_challenges/en/.

Arciniegas, D.B., Anderson, C.A., Topkoff, J., McAllister, T.W., 2005. Mild traumatic brain injury: a neuropsychiatric approach to diagnosis, evaluation, and treatment. Neuropsychiatr. Dis. Treat. 1 (4), 311–327.

Zemek, R., Barrowman, N., Freedman, S.B., Gravel, J., Gagnon, I., McGahern, C., Aglipay, M., Sangha, G., Boutis, K., Beer, D., Craig, W., Burns, E., Farion, K.J., Mikrogianakis, A., Barlow, K., Dubrovsky, A.S., Meeuwisse, W., Gioia, G., Meehan, W.P., Beauchamp, M.H., Kamil, Y., Grool, A.M., Hoshizaki, B., Anderson, P., Brooks, B.L., Yeates, K.O., Vassilyadi, M., Klassen, T., Keightley, M., Richer, L., DeMatteo, C., Osmond, M.H., 2016. Clinical Risk Score for Persistent Postconcussion Symptoms Among Children With Acute Concussion in the ED. JAMA 315 (10), 1014. https://doi.org/10.1001/jama.2016.1203.

Ledoux, A.-A., Tang, K., Yeates, K.O., Pusic, M.V., Boutis, K., Craig, W.R., Gravel, J., Freedman, S.B., Gagnon, I., Gioia, G.A., Osmond, M.H., Zemek, R.L., 2019. Natural progression of symptom change and recovery from concussion in a pediatric population. JAMA Pediatrics 173 (1), e183820. https://doi.org/10.1001/jamapediatrics.2018.3820.

Torres, A. R., Shaikh, Z. I., Chavez, W., & Maldonado, J. E. (n.d.). Brain MRI in children with mild traumatic brain injury and persistent symptoms in both sports- and non-sports-related concussion. *Cureus 11*(1). https://doi.org/10.7759/cureus.3937.

Shenton, M.E., Hamoda, H.M., Schneiderman, J.S., Bouix, S., Pasternak, O., Rathi, Y., Vu, M.-A., Purohit, M.P., Helmer, K., Koerte, I., Lin, A.P., Westin, C.-F., Kikinis, R., Kubicki, M., Stern, R.A., Zafonte, R., 2012. A review of magnetic resonance imaging and diffusion tensor imaging findings in mild traumatic brain injury. Brain Imaging Behav. 6 (2), 137–192. https://doi.org/10.1007/s11682-012-9156-5.

Barlow, K.M., Crawford, S., Brooks, B.L., Turley, B., Mikrogianakis, A., 2015. The Incidence of Postconcussion Syndrome Remains Stable Following Mild Traumatic Brain Injury in Children. Pediatr. Neurol. 53 (6), 491–497. https://doi.org/10.1016/j.pediatrneurol.2015.04.011.

Taylor, H.G., Dietrich, A., Nuss, K., Wright, M., Rusin, J., Bangert, B., Minich, N., Yeates, K.O., 2010. Post-concussive symptoms in children with mild traumatic brain injury. Neuropsychology 24 (2), 148–159. https://doi.org/10.1037/a0018112.

Büki, A., Povlishock, J.T., 2006. All roads lead to disconnection? – Traumatic axonal injury revisited. Acta Neurochir. 148 (2), 181–194. https://doi.org/10.1007/s00701-005-0674-4.

Eierud, C., Craddock, R.C., Fletcher, S., Aulakh, M., King-Casas, B., Kuehl, D., LaConte, S. M., 2014. Neuroimaging after mild traumatic brain injury: Review and meta-analysis. *NeuroImage: Clinical* 4, 283–294. https://doi.org/10.1016/j.nicl.2013.12.009.

Niogi, S.N., Mukherjee, P., 2010. Diffusion tensor imaging of mild traumatic brain injury. J. Head Trauma Rehab. 25 (4), 241–255. https://doi.org/10.1097/HTR.0b013e3181e52c2a.

Einarsen, C.E., Moen, K.G., Håberg, A.K., Eikenes, L., Kvistad, K.A., Xu, J., Moe, H.K., Tollefsen, M.H., Vik, A., Skandsen, T., 2019. Patients with mild traumatic brain injury recruited from both hospital and primary care settings: a controlled longitudinal magnetic resonance imaging study. J. Neurotrauma 36 (22), 3172–3182. https://doi.org/10.1089/neu.2018.6360.

Wilde, E. A., Mccauley, S. R., Hunter, J. V., Bigler, E. D., Chu, Z., Wang, Z. J., Hanten, G. R., Troyanskaya, M., Yallampalli, R., Li, B. X., Chia, J., & Levin, H. S. (2008). *Diffusion tensor imaging of acute mild traumatic brain injury in adolescents Background: Despite normal CT imaging and neurologic functioning, many individuals report*. https://n.neurology.org/content/neurology/70/12/948.full.pdf.

Chu, Z., Wilde, E.A., Hunter, J.V., McCauley, S.R., Bigler, E.D., Troyanskaya, M., Yallampalli, R., Chia, J.M., Levin, H.S., 2010. Voxel-based analysis of diffusion tensor imaging in mild traumatic brain injury in adolescents. Am. J. Neuroradiol. 31 (2), 340–346. https://doi.org/10.3174/ajnr.A1806.

Virji-Babul, N., Borich, M.R., Makan, N., Moore, T., Frew, K., Emery, C.A., Boyd, L.A., 2013. Diffusion tensor imaging of sports-related concussion in adolescents. Pediatr. Neurol. 48 (1), 24–29. https://doi.org/10.1016/j.pediatrneurol.2012.09.005.
Borich, M., Makan, N., Boyd, L., Virji-Babul, N., 2013. Combining whole-brain voxel-wise analysis with in vivo tractography of diffusion behavior after sports-related concussion in adolescents: a preliminary report. J. Neurotrauma 30 (14), 1243–1249. https://doi.org/10.1089/neu.2012.2818.
Mayer, A.R., Ling, J.M., Yang, Z., Pena, A., Yeo, R.A., Klimaj, S., 2012. Diffusion abnormalities in pediatric mild traumatic brain injury. J. Neurosci. 32 (50), 17961–17969. https://doi.org/10.1523/JNEUROSCI.3379-12.2012.
Yallampalli, R., Wilde, E.A., Bigler, E.D., McCauley, S.R., Hanten, G., Troyanskaya, M., Hunter, J.V., Chu, Z., Li, X., Levin, H.S., 2013. Acute white matter differences in the fornix following mild traumatic brain injury using diffusion tensor imaging. J. Neuroimaging 23 (2), 224–227. https://doi.org/10.1111/j.1552-6569.2010.00537.x.
Wu, T.C., Wilde, E.A., Bigler, E.D., Yallampalli, R., McCauley, S.R., Troyanskaya, M., Chu, Z., Li, X., Hanten, G., Hunter, J.V., Levin, H.S., 2010. Evaluating the relationship between memory functioning and cingulum bundles in acute mild traumatic brain injury using diffusion tensor imaging. J. Neurotrauma 27 (2), 303–307. https://doi.org/10.1089/neu.2009.1110.
Messé, A., Caplain, S., Paradot, G., Garrigue, D., Mineo, J.-F., Soto Ares, G., Ducreux, D., Vignaud, F., Rozec, G., Desal, H., Pélégrini-Issac, M., Montreuil, M., Benali, H., Lehéricy, S., 2011. Diffusion tensor imaging and white matter lesions at the subacute stage in mild traumatic brain injury with persistent neurobehavioral impairment. Hum. Brain Mapp. 32 (6), 999–1011. https://doi.org/10.1002/hbm.21092.
Wu, T., Merkley, T.L., Wilde, E.A., Barnes, A., Li, X., Chu, Z.D., McCauley, S.R., Hunter, J. V., Levin, H.S., 2018. A preliminary report of cerebral white matter microstructural changes associated with adolescent sports concussion acutely and subacutely using diffusion tensor imaging. Brain Imaging Behav. 12 (4), 962–973. https://doi.org/10.1007/s11682-017-9752-5.
Yin, B., Li, D.-D., Huang, H., Gu, C.-H., Bai, G.-H., Hu, L.-X., Zhuang, J.-F., Zhang, M., 2019. Longitudinal changes in diffusion tensor imaging following mild traumatic brain injury and correlation with outcome. Front. Neural Circuits 13. https://doi.org/10.3389/fncir.2019.00028.
Bartnik-Olson, B.L., Holshouser, B., Wang, H., Grube, M., Tong, K., Wong, V., Ashwal, S., 2014. Impaired neurovascular unit function contributes to persistent symptoms after concussion: a pilot study. J. Neurotrauma 31 (17), 1497–1506. https://doi.org/10.1089/neu.2013.3213.
Zhang, H., Schneider, T., Wheeler-Kingshott, C.A., Alexander, D.C., 2012. NODDI: practical in vivo neurite orientation dispersion and density imaging of the human brain. NeuroImage 61 (4), 1000–1016. https://doi.org/10.1016/j.neuroimage.2012.03.072.
Palacios, E., Owen, J.P., Yuh, E.L., Wang, M.B., Vassar, M.J., Ferguson, A.R., Diaz-Arrastia, R., Giacino, J.T., Okonkwo, D.O., Robertson, C.S., Stein, M.B., Temkin, N., Jain, S., McCrea, M., Mac Donald, C.L., Levin, H.S., Manley, G.T., Mukherjee, P., Investigators, T.-R.-A.-C.-K.-T.-B.-I., 2018. The evolution of white matter changes after mild traumatic brain injury: a DTI and NODDI study [Preprint]. Neuroscience. https://doi.org/10.1101/345629.
Fukutomi, H., Glasser, M.F., Murata, K., Akasaka, T., Fujimoto, K., Yamamoto, T., Autio, J.A., Okada, T., Togashi, K., Zhang, H., Van Essen, D.C., Hayashi, T., 2018. Does the diffusion tensor model predict the neurite distribution of cerebral cortical gray matter? – Cortical DTI-NODDI [Preprint]. Neuroscience. https://doi.org/10.1101/441659.
Palacios, E.M., Owen, J.P., Yuh, E.L., Wang, M.B., Vassar, M.J., Ferguson, A.R., Diaz-Arrastia, R., Giacino, J.T., Okonkwo, D.O., Robertson, C.S., Stein, M.B., Temkin, N., Jain, S., McCrea, M., MacDonald, C.L., Levin, H.S., Manley, G.T., Mukherjee, P., 2020. The evolution of white matter microstructural changes after mild traumatic brain injury: a longitudinal DTI and NODDI study. Sci. Adv. 6 (32) https://doi.org/10.1126/sciadv.aaz6892.
Churchill, N.W., Caverzasi, E., Graham, S.J., Hutchison, M.G., Schweizer, T.A., 2019. White matter during concussion recovery: comparing diffusion tensor imaging (DTI) and neurite orientation dispersion and density imaging (NODDI). Hum. Brain Mapp. 40 (6), 1908–1918. https://doi.org/10.1002/hbm.v40.610.1002/hbm.24500.
Figaji, A.A., 2017. Anatomical and physiological differences between children and adults relevant to traumatic brain injury and the implications for clinical assessment and care. Front. Neurol. 8 https://doi.org/10.3389/fneur.2017.00685.
Gioia, G.A., Schneider, J.C., Vaughan, C.G., Isquith, P.K., 2009. Which symptom assessments and approaches are uniquely appropriate for paediatric concussion? Br. J. Sports Med. 43 (Suppl 1), i13–i22. https://doi.org/10.1136/bjsm.2009.058255.
Kirkwood, M.W., Yeates, K.O., Wilson, P.E., 2006. Pediatric sport-related concussion: a review of the clinical management of an oft-neglected population. Pediatrics 117 (4), 1359–1371. https://doi.org/10.1542/peds.2005-0994.
Eme, R., 2017. Neurobehavioral outcomes of mild traumatic brain injury: a mini review. Brain Sci. 7 (5), 46. https://doi.org/10.3390/brainsci7050046.
Yeates, K.O., Beauchamp, M., Craig, W., Doan, Q., Zemek, R., Bjornson, B., Gravel, J., Mikrogianakis, A., Goodyear, B., Abdeen, N., Beaulieu, C., Dehaes, M., Deschenes, S., Harris, A., Lebel, C., Lamont, R., Williamson, T., Barlow, K.M., Bernier, F., Brooks, B. L., Emery, C., Freedman, S.B., Kowalski, K., Mrklas, K., Tomfohr-Madsen, L., Schneider, K.J., 2017. Advancing Concussion Assessment in Pediatrics (A-CAP): a prospective, concurrent cohort, longitudinal study of mild traumatic brain injury in children: Protocol study. BMJ Open 7 (7), e017012. https://doi.org/10.1136/bmjopen-2017-017012.
Bialy, L., Plint, A., Zemek, R., Johnson, D., Klassen, T., Osmond, M., Freedman, S.B., 2018. Pediatric emergency research Canada: origins and evolution. Pediatr. Emerg. Care 34 (2), 138–144. https://doi.org/10.1097/PEC.0000000000001360.
Lefevre-Dognin, C., Cogné, M., Perdrieau, V., Granger, A., Heslot, C., Azouvi, P., 2021. Definition and epidemiology of mild traumatic brain injury. Neurochirurgie 67 (3), 218–221. https://doi.org/10.1016/j.neuchi.2020.02.002.
Teasdale, G., Jennett, B., 1974. Assessment of come and impaired consciousness: a practical scale. Lancet 304 (7872), 81–84. https://doi.org/10.1016/S0140-6736(74)91639-0.
Greenspan, L., McLellan, B.A., Greig, H., 1985. Abbreviated injury scale and injury severity score: a scoring chart. J. Trauma Acute Care Surg. 25 (1), 60–64.
Meares, S., Shores, E.A., Taylor, A.J., Batchelor, J., Bryant, R.A., Baguley, I.J., Chapman, J., Gurka, J., Marosszeky, J.E., 2011. The prospective course of postconcussion syndrome: the role of mild traumatic brain injury. Neuropsychology 25 (4), 454–465. https://doi.org/10.1037/a0022580.
Gerring, J.P., Brady, K.D., Chen, A., Vasa, R., Grados, M., Bandeen-roche, K.J., Bryan, R. N., Denckla, M.B., 1998. Premorbid prevalence of ADHD and development of secondary ADHD after closed head injury. J. Am. Acad. Child Adolesc. Psychiatry 37 (6), 647–654. https://doi.org/10.1097/00004583-199806000-00015.
Ware, A. L., Shukla, A., Guo, S., Onicas, A., Geeraert, B. L., Goodyear, B. G., Yeates, K. O., & Lebel, C. (2021). *Participant Factors That Contribute to Magnetic Resonance Imaging Motion Artifacts in Children With Mild Traumatic Brain Injury or Orthopedic Injury*. https://doi.org/10.21203/rs.3.rs-173447/v1.
Tustison, N.J., Cook, P.A., Klein, A., Song, G., Das, S.R., Duda, J.T., Kandel, B.M., van Strien, N., Stone, J.R., Gee, J.C., Avants, B.B., 2014. Large-scale evaluation of ANTs and FreeSurfer cortical thickness measurements. NeuroImage 99, 166–179. https://doi.org/10.1016/j.neuroimage.2014.05.044.
Reynolds, J.E., Grohs, M.N., Dewey, D., Lebel, C., 2019. Global and regional white matter development in early childhood. NeuroImage 196, 49–58. https://doi.org/10.1016/j.neuroimage.2019.04.004.
Benjamini, Y., Hochberg, Y. (1995). Controlling the false discovery rate: a practical and powerful approach to multiple testing. *J. Royal Stat. Soc. Ser. B (Methodological)*, *57* (1), 289–300. JSTOR.
Faul, F., Erdfelder, E., Buchner, A., Lang, A.-G., 2009. Statistical power analyses using G*Power 3.1: tests for correlation and regression analyses. Behav. Res. Methods 41 (4), 1149–1160. https://doi.org/10.3758/BRM.41.4.1149.
Ayr, L.K., Yeates, K.O., Taylor, H.G., Browne, M., 2009. Dimensions of postconcussive symptoms in children with mild traumatic brain injuries. J. Int. Neuropsychol. Soc.: JINS 15 (1), 19–30. https://doi.org/10.1017/S1355617708090188.
Deoni, S.C.L., O'Muircheartaigh, J., Elison, J.T., Walker, L., Doernberg, E., Waskiewicz, N., Dirks, H., Piryatinsky, I., Dean, D.C., Jumbe, N.L., 2016. White matter maturation profiles through early childhood predict general cognitive ability. Brain Struct. Funct. 221 (2), 1189–1203. https://doi.org/10.1007/s00429-014-0947-x.
Storey, J.D., Tibshirani, R., 2003. Statistical significance for genomewide studies. PNAS 100 (16), 9440–9445. https://doi.org/10.1073/pnas.1530509100.
Geeraert, B.L., Lebel, R.M., Lebel, C., 2019. A multiparametric analysis of white matter maturation during late childhood and adolescence. Hum. Brain Mapp. 40 (15), 4345–4356. https://doi.org/10.1002/hbm.24706.
Mah, A., Geeraert, B., Lebel, C., Leemans, A., 2017. Detailing neuroanatomical development in late childhood and early adolescence using NODDI. PLoS One 12 (8), e0182340. https://doi.org/10.1371/journal.pone.0182340.
Zhao, X., Shi, J., Dai, F., Wei, L., Zhang, B., Yu, X., Wang, C., Zhu, W., Wang, H., 2021. Brain development from newborn to adolescence: evaluation by neurite orientation dispersion and density imaging. Front. Hum. Neurosci. 15 https://doi.org/10.3389/fnhum.2021.616132.
Babcock, L., Yuan, W., Leach, J., Nash, T., Wade, S., Suskauer, S., 2015. White matter alterations in youth with acute mild traumatic brain injury. J. Pediatr. Rehabil. Med. 8 (4), 285–296. https://doi.org/10.3233/PRM-150347.
Wilde, E.A., McCauley, S.R., Hunter, J.V., Bigler, E.D., Chu, Z., Wang, Z.J., Hanten, G.R., Troyanskaya, M., Yallampalli, R., Li, X., Chia, J., Levin, H.S., 2008. Diffusion tensor imaging of acute mild traumatic brain injury in adolescents. Neurology 70 (12), 948–955. https://doi.org/10.1212/01.wnl.0000305961.68029.54.
Goodrich-Hunsaker, N.J., Abildskov, T.J., Black, G., Bigler, E.D., Cohen, D.M., Mihalov, L.K., Bangert, B.A., Taylor, H.G., Yeates, K.O., 2018. Age and sex-related effects in children with mild traumatic brain injury on diffusion MRI properties: a comparison of voxelwise and tractography methods. J. Neurosci. Res. 96 (4), 626–641. https://doi.org/10.1002/jnr.24142.
Wilde, E.A., Ware, A.L., Li, X., Wu, T.C., McCauley, S.R., Barnes, A., Newsome, M.R., Biekman, B.D., Hunter, J.V., Chu, Z.D., Levin, H.S., 2018. Orthopedic injured versus uninjured comparison groups for neuroimaging research in mild traumatic brain injury. J. Neurotrauma 36 (2), 239–249. https://doi.org/10.1089/neu.2017.5513.
Fakhran, S., Yaeger, K., Collins, M., Alhilali, L., 2014. Sex differences in white matter abnormalities after mild traumatic brain injury: localization and correlation with outcome. Radiology 272 (3), 815–823. https://doi.org/10.1148/radiol.14132512.
Lancaster, M.A., Olson, D.V., McCrea, M.A., Nelson, L.D., LaRoche, A.A., Muftuler, L.T., 2016. Acute white matter changes following sport-related concussion: a serial diffusion tensor and diffusion kurtosis tensor imaging study. Hum. Brain Mapp. 37 (11), 3821–3834. https://doi.org/10.1002/hbm.23278.
Delic, J., Alhilali, L.M., Hughes, M.A., Gumus, S., Fakhran, S., 2016. White matter injuries in mild traumatic brain injury and posttraumatic migraines: diffusion entropy analysis. Radiology 279 (3), 859–866. https://doi.org/10.1148/radiol.2015151388.
King, R., Grohs, M.N., Kirton, A., Lebel, C., Esser, M.J., Barlow, K.M., 2019. Microstructural neuroimaging of white matter tracts in persistent post-concussion syndrome: a prospective controlled cohort study. NeuroImage: Clinical 23, 101842. https://doi.org/10.1016/j.nicl.2019.101842.
Mac Donald, C.L., Barber, J., Wright, J., Coppel, D., De Lacy, N., Ottinger, S., Peck, S., Panks, C., Sun, S., Zalewski, K., Temkin, N., 2018. Longitudinal clinical and

neuroimaging evaluation of symptomatic concussion in 10- to 14-year-old youth athletes. J. Neurotrauma 36 (2), 264–274. https://doi.org/10.1089/neu.2018.5629.

Manning, K. Y. (2017). Multiparametric MRI changes persist beyond recovery in concussed adolescent hockey players. 15.

Genc, S., Malpas, C.B., Holland, S.K., Beare, R., Silk, T.J., 2017. Neurite density index is sensitive to age related differences in the developing brain. NeuroImage 148, 373–380. https://doi.org/10.1016/j.neuroimage.2017.01.023.

Churchill, N.W., Caverzasi, E., Graham, S.J., Hutchison, M.G., Schweizer, T.A., 2017. White matter microstructure in athletes with a history of concussion: Comparing diffusion tensor imaging (DTI) and neurite orientation dispersion and density imaging (NODDI). Hum. Brain Mapp. 38 (8), 4201–4211. https://doi.org/10.1002/hbm.23658.

Giza, C.C., Hovda, D.A., 2014. The new neurometabolic cascade of concussion. Neurosurgery 75 (0 4), S24–S33. https://doi.org/10.1227/NEU.0000000000000505.

Post, A., Hoshizaki, T. B., Zemek, R., Gilchrist, M. D., Koncan, D., Dawson, L., Chen, W., Ledoux, A.-A., Pediatric Emergency Research Canada (PERC) 5P Concussion Team. (2017). Pediatric concussion: Biomechanical differences between outcomes of transient and persistent (> 4 weeks) postconcussion symptoms. *J. Neurosurg. Pediatrics*, *19*(6), 641–651. https://doi.org/10.3171/2016.11.PEDS16383.

Haarbauer-Krupa, J., Arbogast, K.B., Metzger, K.B., Greenspan, A.I., Kessler, R., Curry, A. E., Bell, J.M., DePadilla, L., Pfeiffer, M.R., Zonfrillo, M.R., Master, C.L., 2018. Variations in mechanisms of injury for children with concussion. J. Pediatr. 197, 241–248.e1. https://doi.org/10.1016/j.jpeds.2018.01.075.

Raizman, R., Tavor, I., Biegon, A., Harnof, S., Hoffmann, C., Tsarfaty, G., Fruchter, E., Tatsa-Laur, L., Weiser, M., Livny, A., 2020. Traumatic brain injury severity in a network perspective: a diffusion MRI based connectome study. Sci. Rep. 10 (1), 9121. https://doi.org/10.1038/s41598-020-65948-4.

Iraji, A., Chen, H., Wiseman, N., Zhang, T., Welch, R., O'Neil, B., Kulek, A., Ayaz, S.I., Wang, X., Zuk, C., Haacke, E.M., Liu, T., Kou, Z., 2016. Connectome-scale assessment of structural and functional connectivity in mild traumatic brain injury at the acute stage. NeuroImage: Clinical 12, 100–115. https://doi.org/10.1016/j.nicl.2016.06.012.

Palacios, E.M., Martin, A.J., Boss, M.A., Ezekiel, F., Chang, Y.S., Yuh, E.L., Vassar, M.J., Schnyer, D.M., Mac Donald, C.L., Crawford, K.L., Irimia, A., Toga, A.W., Mukherjee, P., 2017. Towards precision and reproducibility of diffusion tensor imaging: a multicenter diffusion phantom and traveling volunteer study. AnJNR. Am. J. Neuroradiol. 38 (3), 537–545. https://doi.org/10.3174/ajnr.A5025.